18th World Conference on Nondestructive Testing, 16-20 April 2012, Durban, South Africa

Simulation of ultrasonic guided wave inspection in CIVA software platform

Bastien CHAPUIS [1], Karim JEZZINE [1], Vahan BARONIAN [1], Damien SEGUR [1], Alain LHEMERY [1]

[1] CEA, LIST, F-91191 Gif-sur-Yvette, France
bastien.chapuis@cea.fr

Abstract
The use of Guided Waves (GW) is a potentially attractive solution to inspect large structures from a single measurement point thanks to the capability of these waves to propagate over large distances. However, the multimodal and dispersive nature of GW makes it difficult to analyze and interpret the signals. This has motivated the development at CEA LIST of a simulation tool dedicated to GW NDT implemented in the CIVA software. A general formulation has been derived from the reciprocity theorem, which allows simulating the complete GW NDT response in a modal decomposition. The simulation tool is divided in three modules and the guiding structures that can be addressed are plates and tubes, possibly multilayered. The first module allows modes computation, the second module computation of the field radiated by a transducer and the third module the full response of GW NDT control. Comparisons to literature and experimental data are provided and the developments in progress at CEA LIST in order to extend the capability of the GW NDT simulation tool are also presented.

Keywords: Guided waves, SAFE method, simulation, CIVA software

1. Introduction

The use of Guided Waves (GW) is an attractive solution for inspecting large structures since these waves can propagate over long distances and thus examine large zones without moving the transducer. Typical applications of GW rise from plate like structures, for example aircraft fuselage [1], through rail [2] to pipes in various industries [3]. GW can also be very convenient when the structure to be inspected presents accessibility problems. However, GW are multimodal and dispersive, and these characteristics lead to difficulties for practical implementation of the technique. Indeed, GW signals are generally very complex to analyze and to interpret and therefore require a high degree of expertise to be exploited [4].
This context has motivated CEA LIST to develop simulation tools for predicting GW NDT. These tools are integrated into CIVA software platform and aim at helping engineers and researchers in the set-up of GW testing configurations with three modules, each dedicated to the different steps of an examination. The first module gives the possibility to compute the modes which are likely to propagate in the waveguide using the SAFE (Semi Analytical Finite Element) method [5]. Several possibilities are offered to visualize the properties of these modes. The second module is dedicated to transducer design in order to optimize their sensitivity to desired modes. The radiated field from different type of transducers (contact with or without wedge, surrounding or surrounded arrays in tube, with phased arrays capabilities and different loading directions) can be studied. The last module allows simulating the full response of a NDT examination in pulse-echo or pitch-catch configurations.
The theory behind the simulation tools is briefly described in a first part of this paper. Then, the capabilities of the guided waves simulation tools are presented through various examples.

2. Theory

GW are multimodal. That is to say that in a given structure several modes can propagate and interact with a potential defect, leading to complex signals. The computing strategy implemented in CIVA is based on a modal approach and post-processing of these modes to account for transducer diffraction effects and flaw scattering. This strategy, derived from the reciprocity theorem, is very efficient in term of computation time. The simulations tools can then be used intensively, which is compatible with industrial needs.

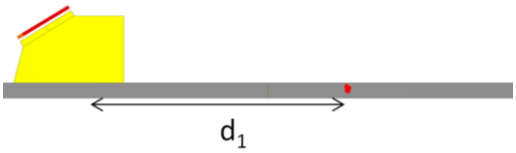

Figure 1: Pulse-echo configuration.

According to the reciprocity theorem proposed by Auld [6], the frequency dependent signal s_1 measured by the transducer in the pulse-echo configuration depicted in Figure 1 can be written as:

$$s_1(\omega) = \frac{-i\omega}{P} \sum_n \sum_m A_n^r A_m^e R_{nm} exp(-i(\beta_n + \beta_m) d_1) \quad (1)$$

where P is the electrical power provided to the transducer and ω the angular frequency. A_m^e and A_n^r are respectively the amplitude of mode m radiated by the transducer and the amplitude of sensitivity to mode n of the transducer in reception; they stand for transducer diffraction effects. R_{nm} is the reflection coefficient for the incident mth mode and the reflected nth mode; they stand for the scattering by an inhomogeneity of the guide. d_1 denotes the distance between the emitter and the scattering zone. This distance appears together with β_n and β_m, the wave number of the nth and mth modes of the guide, in exponential terms which are propagators of GW in the guide. Note that a similar formulation can be established in the case of a pitch-catch configuration.

2.1 SAFE computation of modes

The first step of the simulation is therefore based on the determination of the modes likely to propagate in the structure, which is an essential step for understanding the complex phenomena that occur in a waveguide. This is done using a Semi-Analytical Finite Element (SAFE) method well-established in the literature. In few words, this method involves a finite element computation in the guide section, allowing the computation of the wave numbers β_n that appears in Eq. (1). Other characteristics of modes such as their shape, their attenuation... can be determined. The propagation is otherwise accounted for by means of analytic propagators in the guiding direction normal to the section considered, at no computational cost (same function whatever the range). In Eq. (1), this model gives the solution for the exponential propagator terms.

2.2 Transducer diffraction

For each the type of transducer used (piezoelectric, EMAT,...), it is necessary to derive models adapted to the transduction that takes place. This problem is addressed in the literature for various cases of industrial interest (see Ref. [7] for example). Up to now the models deal with piezo-transducers (with or without wedge) assumed to be sources of normal or tangential

stresses all over their active surface. In Eq. (1), these models give the solution for the terms A_m^e and A_n^r.

2.3 Local models of scattering by defects and by guide discontinuities

Computing the scattering by a guide inhomogeneity is a difficult task. Contrary to bulk waves used in NDT, guided waves have a wavelength often comparable with dimensions of the guide section and with the size of inhomogeneities. In the former case, scattering can be computed by means of approximations (high frequency); in the latter, deriving suitable approximations is almost impossible. Our aim is to write the solution of the scattering problem in the form of a matrix of complex coefficients reflection R_{nm} coefficients in Eq. (1), assuming that modal solutions in guiding structures connected to the local zone of scattering are known. A first method was proposed for planar crack-like defects of arbitrary shape in an otherwise homogeneous guide, assuming that crack surface belongs to the guide cross-section [8]. To deal with arbitrary flaw shapes or guide inhomogeneities, an original finite element (FE) scheme has been developed with the further goal to limit the computation zone to a minimal size for efficiency. The computation zone being necessarily of finite size, its boundaries with all the guiding structures connected to it must be transparent for elastic waves: they must not reflect the incoming waves nor reflect outgoing waves. The extensive description of this method, beyond the scope of this article, is provided in Refs. [9, 10]. However it is important to mention that this very general and efficient formulation is fully compatible with the other steps of Eq. (1). It allows therefore the computing of a GW scattering by any arbitrary defect.

3. Simulation of guided wave inspection in CIVA software

In this paragraph we describe through various examples the capabilities in terms of GW NDT simulation of the guided waves simulation modules. The computational steps follow the logic presented in the previous part and are available in three different modules. First is described the computation of the modes likely to propagate in the structure in order to select the most appropriate one for the examination. Then, the computation of the field radiated by a given transducer is presented. This could help the user to optimally design a sensor or to use it the most appropriately. Finally, the signal measured by a transducer in a realistic testing configuration is computed and analyzed.

3.1 Mode computation

The mode computation is available for planar geometries or tubes. The material is, presently , assumed to be isotropic, but it can be multilayered and viscoelastic. The influence of the presence of a protective layer of a steel pipe on modes in the pipe is presented as an example. The geometry of the structure is entered in a first frame of the CIVA interface. In this example the structure is multilayered, the thickness of the protective layer is chosen as 0.508 mm over a 6.02 mm thick steel tube (Figure 2.a). The properties of the materials are entered in a second frame. The bulk wave velocities of the two materials as well as their density are necessary for the computation of modes (Figure 2.b and c). The protective layer being a viscoleastic coating, the bulk wave attenuations must also be given (Figure 2.c).

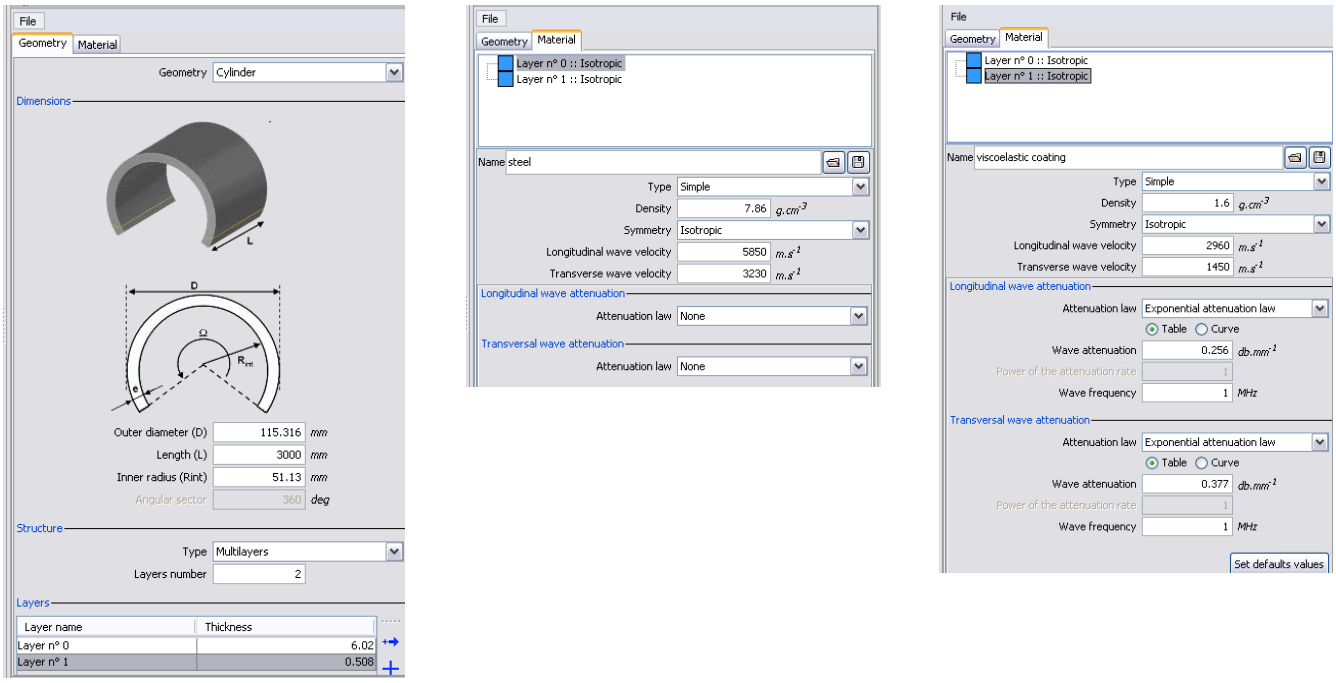

(a) (b) (c)

Figure 2: (a) Description of the geometry, (b) material parameters for the steel pipe and (c) material parameters for the viscoelastic protective layer.

The results are shown in Figure 3, restricted to axisymmetric modes for clarity. At low frequencies, the velocities of the modes are not disturbed by the coating. However, the viscoelasticy of the protective layer introduces damping for the mode encircled in magenta (0.05 dB/m at 110 kHz) which is important to determine in order to estimate the maximal distance that this mode can cover without being of too low amplitude to be detected. At higher frequencies, the influence of the protective layer is more important. For example the mode encircled in green is strongly affected by the coating. Indeed, it can be shown that it is a mode propagating only in the thin epoxy layer, therefore absolutely not suitable for detecting defect in the steel pipe.

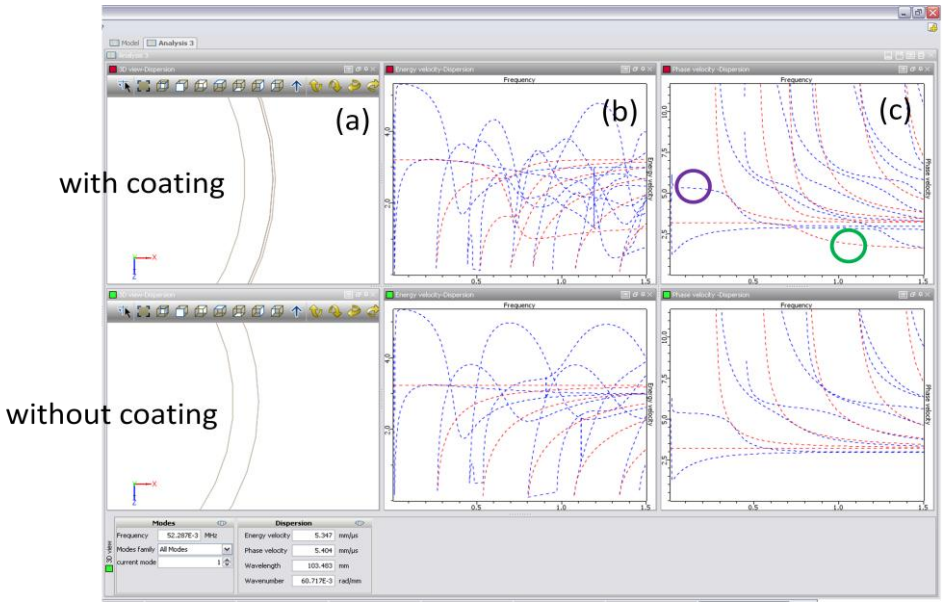

Figure 3: Axisymmetric modes propagating in a steel pipe with and without coating. (a) Zoom of the 3D view of the structure, (b) energy velocity of the modes and (c) phase velocity of the modes.

The validity of the mode computation step has been extensively checked by comparison of its predictions with both experimental and other simulation results as presented in Figure 5 for a viscoelastic isotropic plate of high performance polyethylene (HPPE) 12.7 mm thick for which the dispersion curves are presented in Ref. [11]. The characteristics of this material are given in Figure 4.

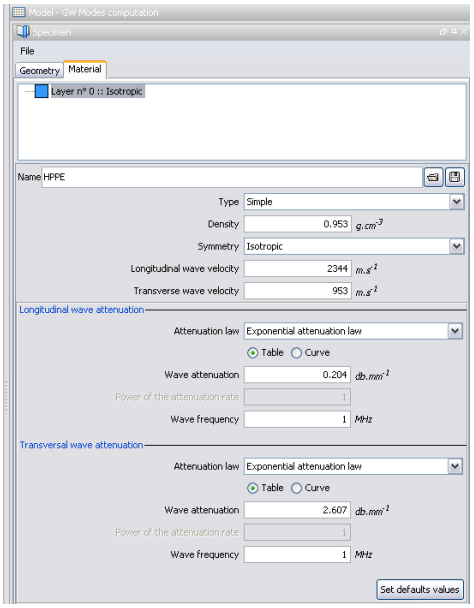

Figure 4: Material coefficient for the HPPE plate given in [11].

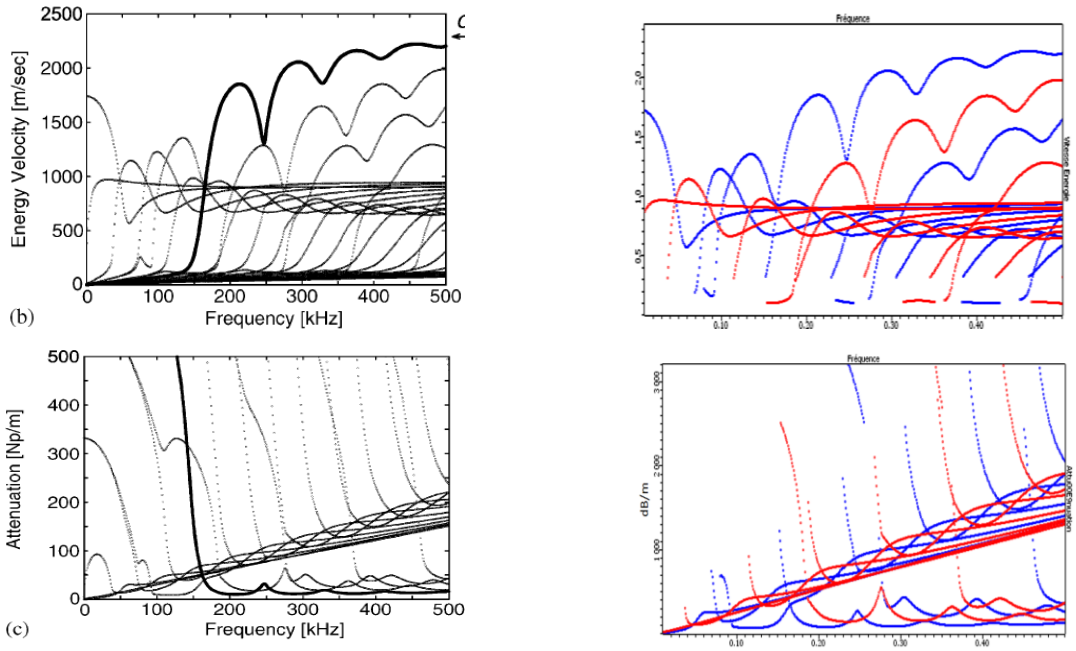

Figure 5: Comparison between results presented in [11] (left) and those given by CIVA (right).

3.2 Field computation

The second module is dedicated to the computation of the field radiated by a transducer. The first example given here is that of a wedge transducer used by Terrien [12] to detect corrosion in plate like structures. The structure is a 2 mm thick aluminium plate and the transducer is a piezoelectric element mounted on a plexiglass wedge with an incident angle of 68°. The transducer has a centre frequency of 2.25 MHz and the incident signal is a 5 cycle toneburst. In Terrien's experiment, the normal displacement at the surface of the plate at a distance of 420 mm from the transducer is measured with a laser probe.

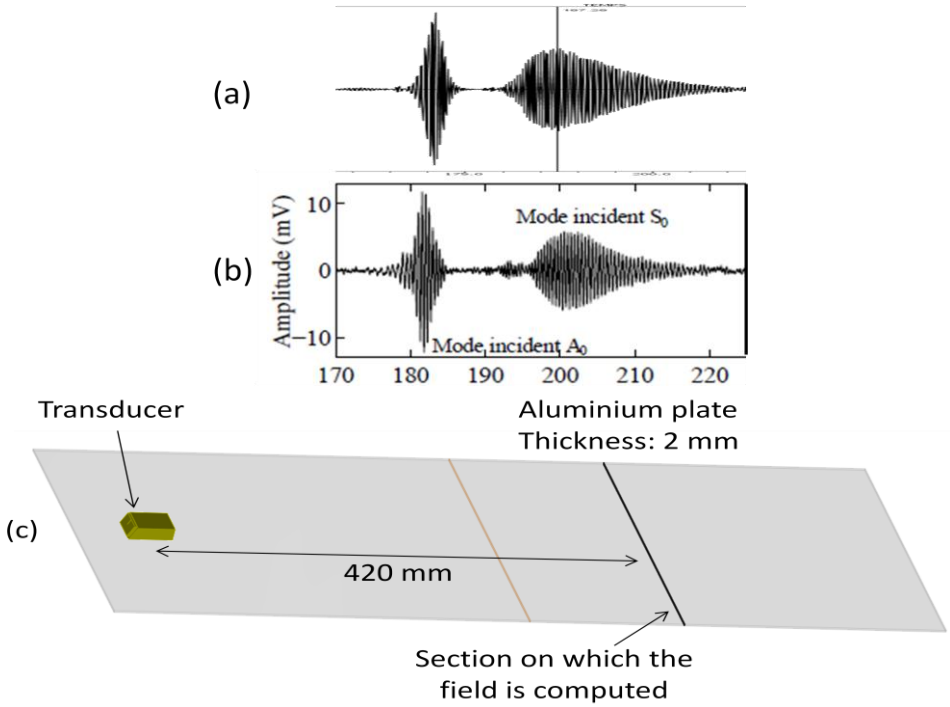

Figure 6: Signal emitted by a wedge transducer in a 2 mm thick aluminium plate at 2.25 MHz and measured by a laser probe at 420 mm from the source. The A_0 and S_0 modes are emitted. Comparison between (a) results given by CIVA and (b) experimental measurements from Terrien [12]. (c) 3D view of the configuration in CIVA.

Another example shows the complexity of the signals that must be addressed by the simulation, even in a simple configuration of transmission between two point-like transducers in a plate [13]. The multimodal aspect of the guided waves is revealed by the different wavepackets propagating at different velocities in the plate (Figure 7). Figure 8 presents the modal energy radiated in the bandwidth of the transducer of Figure 7. These curves are a very useful tool to design sensors specifically sensitive to a particular mode.

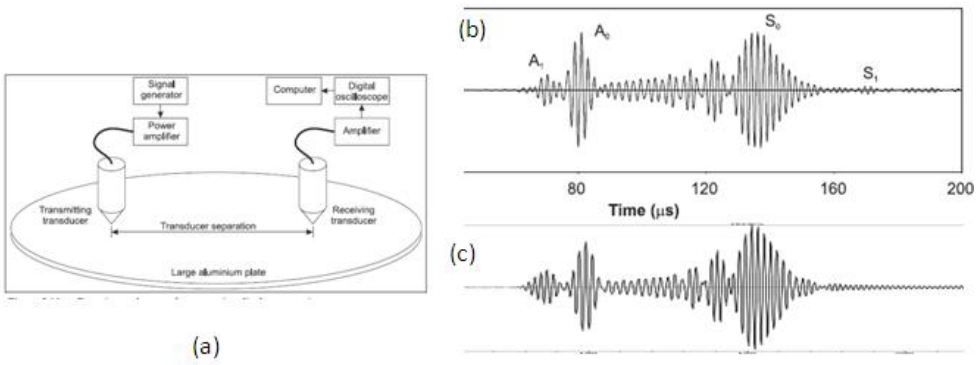

Figure 7: Transmission between two point like transducers in a 5 mm thick aluminium plate excited with a 5 cycle toneburst at 0.5 MHz. (a) Scheme of the experimental setup, (b) experimental signal measured by Wilcox [13] and (c) signal simulated by CIVA.

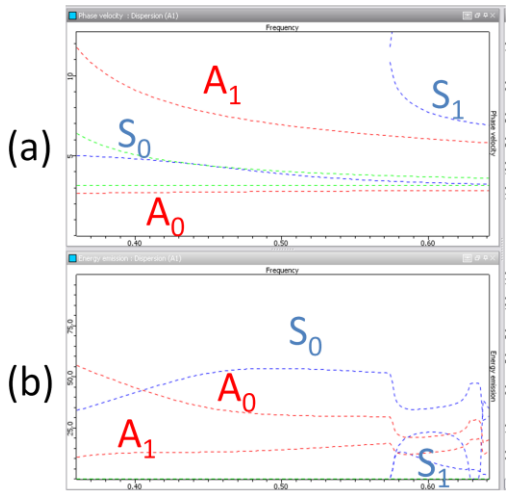

Figure 8: (a) Phase velocities and (b) coefficients of modal energy radiated calculated by CIVA in the bandwidth of the transducer.

The last example illustrates phased array capabilities of the software. A phased-array is considered focusing in a 273.05 mm outer diameter and 9.398 mm thickness steel pipe. The array is an annular array composed of 8 eight elements used to excite guided waves (Figure 9). Delay and amplitude laws determined in [14] are used to focus energy at 1.5 m from the source at a defined radial position. The radiated field is shown in Figure 10 that confirms the focusing of the guided waves. In the next section the same configuration will be used to detect a crack.

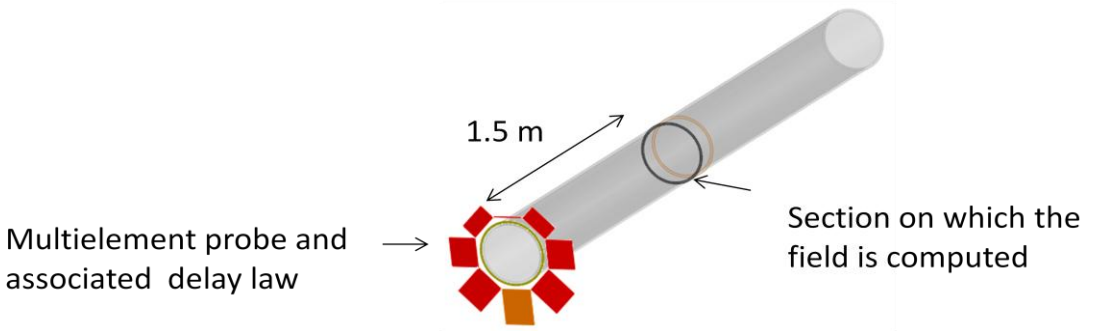

Figure 9: CIVA 3D view of a defect response configuration in a tube. The probe is an annular array of 8 elements, on which amplitude and delay laws are applied.

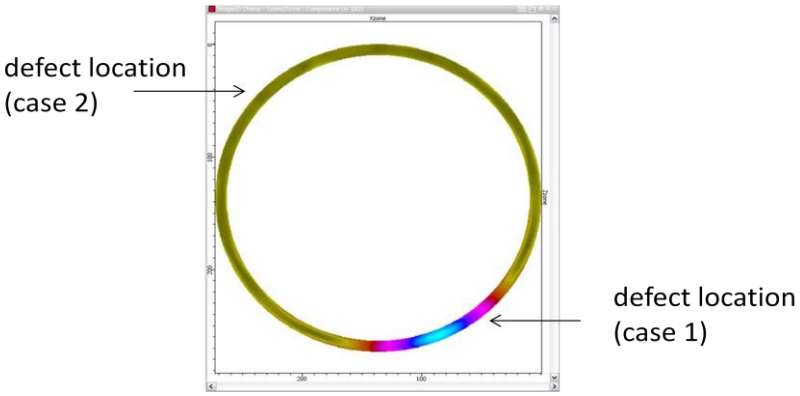

Figure 10: Field computation (Uy axial component) in a section of the tube at 1.5 m from the source.

3.3 Defect response computation

The defect response computation is up to now restricted to the response of a crack normal to the surface of the guide. In a tube the defect can therefore only be a crack perpendicular to the guide axis, but its dimensions are arbitrary: it may be defined as a sectorial ring.

A comparison with literature results is presented in Figure 11. CIVA responses are compared to the simulations described by Li-Guo [15]. Two PZT rings are used to excite longitudinal modes at 100 kHz in the same tube as the last example. A very small (compared to the wavelength) PZT is used as a receiver, in a pitch-catch reflection configuration. The defect simulated by Li-Guo is a notch of 4 mm width and full circumferential extent. In CIVA the defect is a crack (that is to say a notch of very small width) of full circumferential extent. The simulations are performed for various defect height/tube thickness (d/h) ratios. The excellent agreement between both simulations shows that in that case, notch and crack have almost the same response. This is due to the fact that in that configuration the incident wavelength is large compared to the width of the notch.

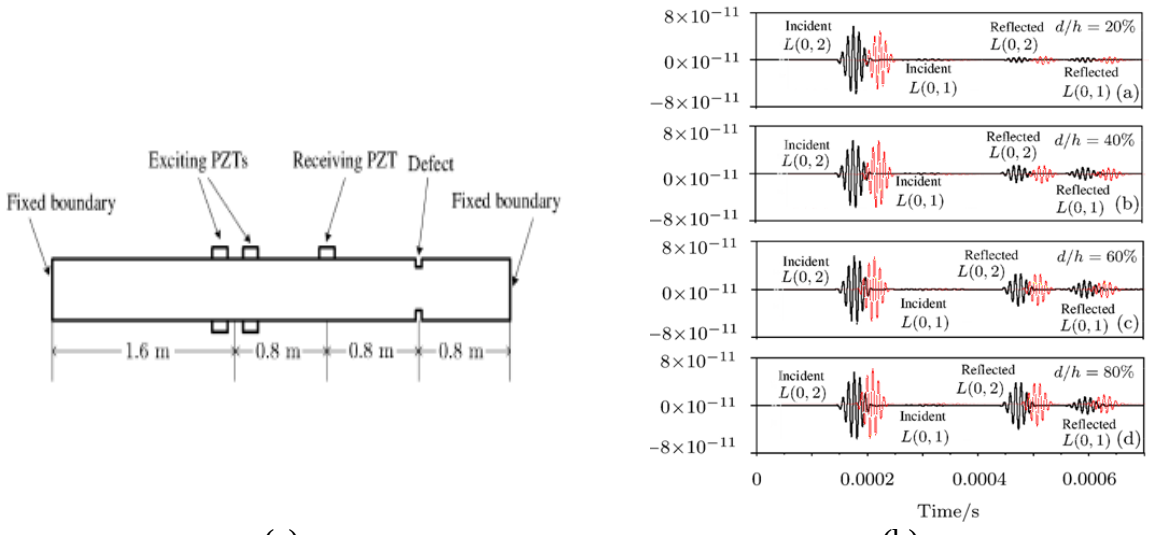

(a) (b)

Figure 11: (a) Configuration of the simulation and (b) signal simulated by Li-Guo [15] (black) and given by CIVA (red) for different defect height/tube thickness (d/h) ratios. The signals given by CIVA are time shifted for clarity.

Phased array focusing capabilities presented in the previous paragraph allows locating the radial position of a non axisymmetric defect. The responses for a 30° angular crack (d/h=100%) situated at 1.5 m from the source for two opposite radial positions shown in Figure 12 (and Figure 10) are simulated and presented in Figure 13. The delay and amplitude laws are used both for radiation and reception in this pulse-echo measurement. When the defect is located at the position of the maximum of the guided wave field the response is (logically) maximal, 26 dB higher than that for the opposite case.

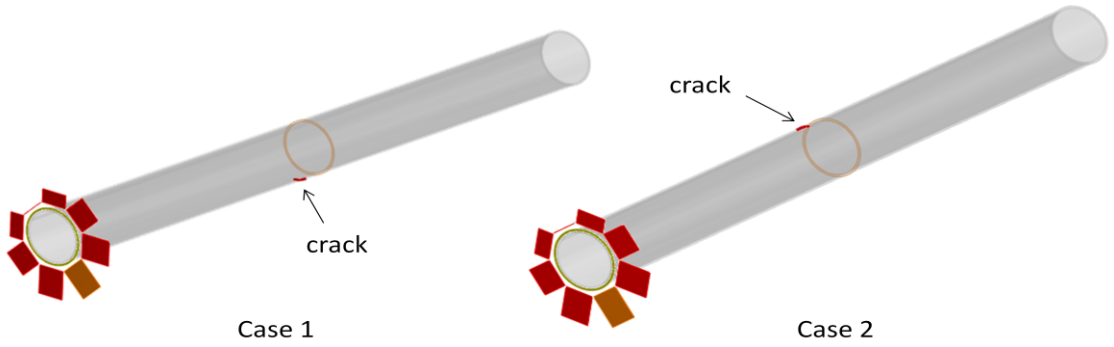

Figure 12: Position of the defect in the pipe.

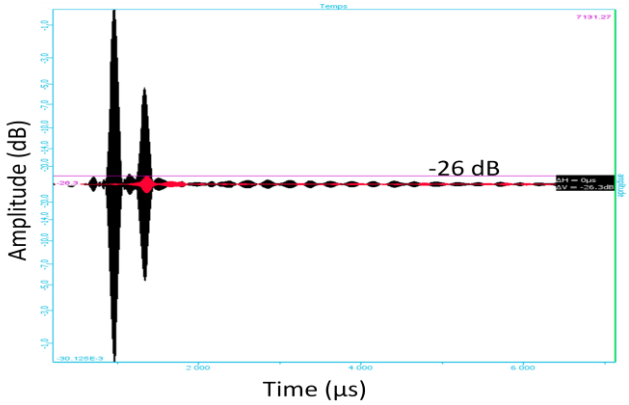

Figure 13: Simulated Ascans for case 1 (black) and case 2 (red).

5. Conclusion and perspectives

The modelling approach for GW/NDT simulation implemented in the CIVA software has been described: wavefields in guides are decomposed on modes and a general formulation allows separating the computation of phenomena typical of GW measurements in different steps. The SAFE method is used for the determination of the modes likely to propagate in uniform guides. GW scattering can be computed in some simple cases (crack normal to the propagation axis) by a scheme derived from the SAFE method, similarly to transducer diffraction effects. Several examples were given to illustrate the capabilities of the CIVA software to simulate a complete GW NDT testing.

Within the same theoretical framework, several extensions are in progress. The waveguide geometry will not be restricted only to tubes and plates but extended to 2D CAD geometries. A specific FE method has been derived for computing the scattering by arbitrary inhomogeneities; it includes exact transparent artificial boundaries for minimizing the size of the FE zone, thus reducing computational costs. This very general and efficient tool will be proposed in the next versions of the CIVA software. GW generation by EMAT in ferromagnetic materials is also being modelled.

References

1. H. Matt, I. Bartoli, and F. Lanza di Scalea, 'Ultrasonic guided wave monitoring of composite wing skin-to-spar bonded joints in aerospace structures', J. Acoust. Soc. Am., Vol 118, pp 2240-2252, 2005.
2. J. Rose, M. Avioli, P. Mudge and R. Sanderson, 'Guided wave inspection potential of defects in rail', NDT & E International, Vol 37, pp 153-161, 2004.
3. M. Lowe and P. Cawley, 'Long Range Guided Wave Inspection Usage – Current Commercial Capabilities and Research Directions', Imperial College, 2006
4. P. Cawley, 'Practical Long Range Guided Wave Inspection – Managing Complexity', Review of Progress in QNDE, Vol 22, pp 22-37, 2003.
5. S.B. Dong and R.B. Nelson, 'On Natural Vibrations and Waves in Laminated Orthotropic Plates', J. Appl. Mech., Vol 39, pp 739-745, 1972.
6. B. Auld, 'General Electromechanical Reciprocity Relations Applied to the Calculation of Elastic Wave Scattering Coefficients', Wave Motion, Vol 1, pp 3-10, 1979.
7. X. Jia, 'Modal analysis of Lamb wave generation in elastic plates by liquid wedge transducers', J. Acoust. Soc. Am., Vol 101, pp 834-842, 1997.
8. K. Jezzine and A. Lhémery, 'Simulation of Guided Wave Inspection Based on the Reciprocity Principle and the Semi-Analytical Finite Element Method', Review of Progress in QNDE, Vol 26, pp 39-46, 2007.
9. V. Baronian, A. Lhémery and K. Jezzine, 'Hybrid SAFE/FE Simulation of Inspections of Elastic Waveguides Containing Several Local Discontinuities or Defects', Review of Progress in QNDE, Vol 30, pp 183-190, 2011.
10. V. Baronian, A.-S. Bonnet-BenDhia and É. Lunéville, 'Transparent Boundary Conditions for the Harmonic Diffraction Problem in an Elastic Waveguide', J. Comput. Appl. Math., Vol 234, pp 1945-1952, 2009.
11. I. Bartoli, A. Marzani, F. Lanza di Scalea and E. Viola, 'Modeling wave propagation in damped waveguides of arbitrary cross-section', J. of Sound and Vib., Vol 295, pp 685-707, 2006.
12. N. Terrien, D. Osmont, D. Royer, F. Lepoutre and A. Déom, 'A combined finite element and modal decomposition method to study the interaction of Lamb modes with micro-defects', Ultrasonics, Vol 46, pp 74-88, 2007.
13. P. Wilcox, 'Lamb wave inspection of large structures using permanently attached transducers', PhD thesis, Imperial College, 1998.
14. W. Luo, J.L. Rose, J.K. Van Velsor and J. Mu, 'Phased array focusing with longitudinal guided waves in a viscoelastic coated hollow cylinder', Review of Progress in QNDE, Vol 25, pp 869-876, 2006.
15. T. Li-Guo, C. Jian-Chun and X. Xiao-Mei, 'Mechanism of the excitation of single pure mode L(0,2) and its interaction with the defect in a hollow cylinder', Chinese Physics, Vol 16, pp 1062-1071, 2007.